NANO LETTERS

2007
Vol. 7, No. 8
2267−2271

Wire versus Tube: Stability of Small One-Dimensional ZnO Nanostructures

Xiao Shen,*,† Philip B. Allen,† James T. Muckerman,‡ James W. Davenport,§ and Jin-Cheng Zheng||

Department of Physics and Astronomy, Stony Brook University, Stony Brook, New York 11794-3800, Chemistry Department, Brookhaven National Laboratory, Upton, New York 11973-5000, Computational Science Center, Brookhaven National Laboratory, Upton, New York 11973-5000, and Center for Functional Nanomaterials, Brookhaven National Laboratory, Upton, New York 11973-5000

Received April 3, 2007; Revised Manuscript Received June 5, 2007

ABSTRACT

This paper presents first-principles calculations for ultrasmall ZnO one-dimensional nanostructures. The calculations were done on ZnO nanowires and single-walled nanotubes with *n* atoms per periodic unit, where one periodic unit is made up of two ZnO layers. The calculations show that, for small *n*, a single-walled nanotube has lower energy than a nanowire. A crossover point near $n = 38$ is predicted. Vibrations and vibrational entropy of competing structures is discussed.

ZnO is an important material because of its electron mobility, wide band gap, and large exciton binding energy. ZnO nanostructures such as nanowires, nanotubes, and nanobelts are promising building blocks for optical, electronic, and chemical sensing devices.[1−3] Several synthetic routes have yielded multiwalled ZnO nanotubes.[4−11] These tubes are 20−450 nm in diameter and have wall thicknesses of 4−100 nm. No single-walled ZnO nanotubes (SWZONTs) have been reported experimentally, although some groups have predicted their properties theoretically.[12,13] Ref 13 also suggested some applications of SWZONTs. Recently, sequences of $(ZnO)_n$ clusters were studied by B. L. Wang et al.[14] They found that tubular structures are metastable for $(ZnO)_n$ ($n = 9−18$) and suggested that ZnO nanotubes resemble C or BN nanotubes. Here we calculate the energy of small ZnO nanowires and SWZONTs with same number of atoms, and find that SWZONTs are energetically more stable at small size. This provides a new guideline for making SWZONTs.

Our nanowires are fragments of wurtzite ZnO, cut along the (001) axis with period *c*. They have 12, 20, 26, 32, and 48 atoms per unit cell, corresponding to C_{6v}, C_{2v}, C_{3v}, C_{2v}, and C_{6v} symmetries (see Figure 1). The SWZONTs are all the zigzag type, which has the same periodicity as the nanowires. We consider the (3,0), (5,0), (6,0), (7,0), (8,0), and (12,0) nanotubes, which correspond to 12, 20, 24, 28, 32, and 48 atoms per unit cell. The surface atoms are not saturated by foreign atoms. Figure 1 shows the cross sections of calculated nanowires and nanotubes.

The calculation uses the plane-wave pseudopotential method, density functional theory (DFT), and the Quantum Espresso/PWSCF code.[15] We use Vanderbilt ultrasoft pseudopotentials[16] with the Perdew−Burke−Ernzerhof (PBE)[17] version of the generalized gradient approximation (GGA) exchange-correlation functional. The Zn 4s and 3d states and O 2p and 2s states are treated as valence electrons. The cutoff of kinetic energy is 30 Ry, while the cutoff of charge density is 300 Ry. The Broyden−Fletcher−Goldfarb−Shanno (BFGS) method is used for geometry optimization. A $5 \times 5 \times 5$ *k*-point mesh is used to test the ZnO bulk properties, and a $1 \times 1 \times 10$ mesh is used for the nanowire and nanotube. We apply Gaussian broadening with smearing parameter 0.002 Ry. The force on each atom is converged to 0.003 eV/Å for all optimizations. We arranged the ZnO nanowires and tubes in a 2D hexagonal supercell and separated them by at least 8 Å. Both internal coordinates of atoms and the lattice constant *c* are relaxed.

The calculated bulk properties are in Table 1 and agree with other GGA calculations, although our results show slightly more underbinding. This may come from ultrasoft pseudopotentials because the plane-wave cutoff and *k*-point sampling convergence are well tested. Our lattice parameters are 2% larger than the experimental values, which is usual for GGA calculations. Both wires and tubes are semiconducting, but the theoretical gap is far too small, as is also

* Corresponding author. Email: xshen@ic.sunysb.edu.
† Department of Physics and Astronomy, Stony Brook University.
‡ Chemistry Department, Brookhaven National Laboratory.
§ Computational Science Center, Brookhaven National Laboratory.
|| Center for Functional Nanomaterials, Brookhaven National Laboratory.

10.1021/nl070788k CCC: $37.00
Published on Web 07/03/2007

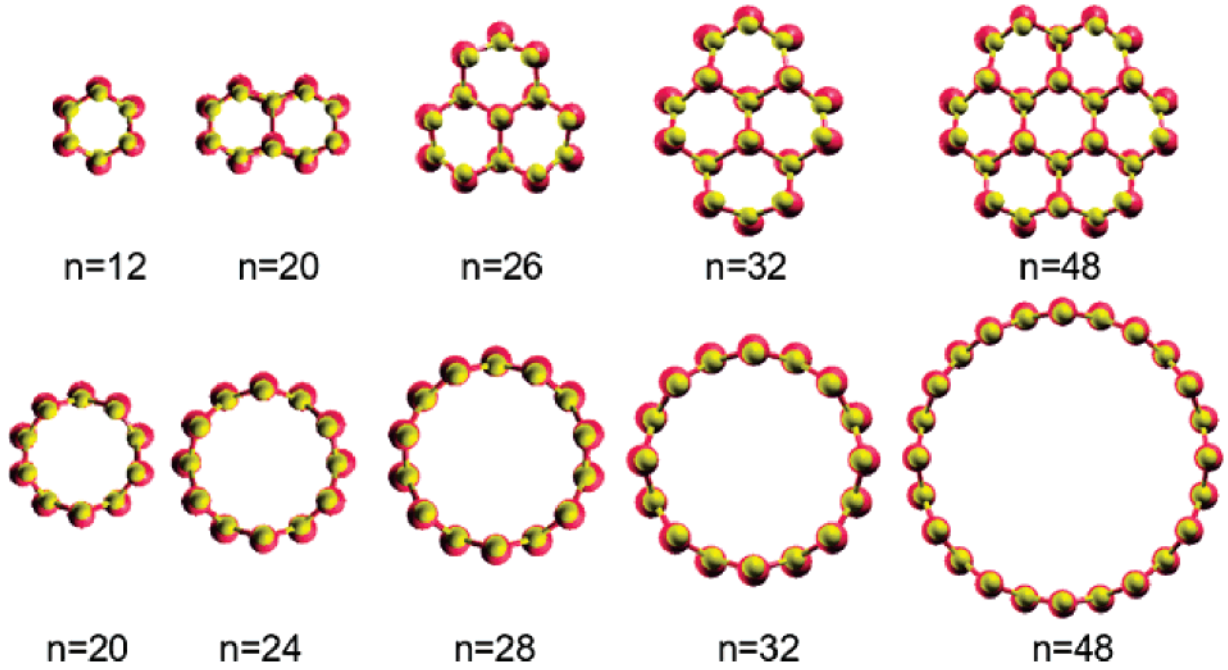

Figure 1. Calculated ZnO nanowires and SWZONTs. Small yellow balls represent Zn atoms, and large orange balls represent O atoms. n is the number of atoms in one periodic unit.

Table 1. Comparison between Our Bulk Results and Other GGA Calculation and Experiments

	present work	other GGA	experiment
a (Å)	3.292	3.283[19]	3.250[21]
c (Å)	5.309	5.289[19]	5.207[21]
u^a	0.3793	0.378[19] 0.3790[20]	0.3817[22]
E_{coh} (eV/fu)	7.27	7.692[20]	7.56[22]
B_0 (GPa)	127	149[19], 133.7[20]	142.6[23]
band gap (eV)	0.71	0.75[19]	3.4[24]

[a] The spacing between closest Zn and O layers is $(^1/_2 - u)c$.

true for bulk ZnO (see Table 1). Previous work[12] calculated the (4,4) armchair SWZONT and suggested that armchair SWZONTs act like conductors. We tested this and found a positive band gap similar to zigzag SWZONTs.

In our calculation, the nanowires are pieces of bulk ZnO. The exposed surfaces correspond to $(10\bar{1}0)$ and $(11\bar{2}0)$ nonpolar surfaces of wurtzite ZnO. For a review of ZnO surfaces, see ref 18. One issue that may arise is whether there could be surface reconstructions apart from ordinary relaxations. To the best of our knowledge, for those surfaces, no reconstructions are reported, except (1×1), whose features are the tilting and contraction of surface Zn−O bonds, which are also observed in our calculation. We also did a direct test for the possibility of a (1×2) surface reconstruction in $n = 26$ nanowire. We took a fully relaxed nanowire, doubled the unit cell along the c-axis, and gave every atom a random displacement between 0 and 0.2 Å. For three different starting displacements, the final geometry is the same as the undisplaced one. No dimerization is observed.

The first nanowire (12 atoms per unit cell) is also the first nanotube. For the second nanowire (two honeycomb units, 20 atoms per cell), we found that the nanowire structure is higher in energy than the SWZONT. To test whether the relative stability depends on the choice of exchange-correlation functional, we changed GGA to LDA (Perdew−Zunger)[25] for the 20 atoms per cell C_{2v} nanowire and (5,0) nanotube. The results show that the SWZONT is indeed more stable, although the difference of energies changed from ∼90 to ∼60 meV. Figure 2 shows the total energy (measured from the global minimum, E_0) vs lattice parameter c for both GGA and LDA results.

Larger nanowires and SWZONTs are also calculated. The final energies of relaxed nanowires and nanotubes are plotted in Figure 3. It shows that, for 1D ZnO structures ($\lesssim$38 atoms per unit cell), the SWZONT is energetically more favorable than the crystal-like nanowire form. This can be understood if we view ZnO bonds as covalent. The wurtzite ZnO crystal has σ bonds made from sp^3 hybrid orbitals. Small nanowires have dangling bonds on the surface that increase the energy. In a nanotube, as in a graphene-like planar sheet, π bonds resulting from sp^2 hybridization will form, lowering the energy. As the wire grows larger, the fraction of surface dangling bonds decreases and the fraction of saturated sp^3 σ bonds increases, so the wire will eventually have lower energy than the SWNT.

The total energy $E_{NT}(n)$ of a SWZONT with n atoms in the unit cell can be written as the sum of total energy of graphene-like planar ZnO sheet E_{sheet} and a strain energy $E_{strain}(n)$ related to tube curvature,

$$E_{NT}(n) = E_{sheet} + E_{strain}(n)$$

For a single-layer planar ZnO sheet, we find $E_{sheet} = 440$ meV/pair relative to bulk ZnO. The strain energy for a nanotube is related to radius R by $E_{strain}(n) \approx c/R^2$.[26] The

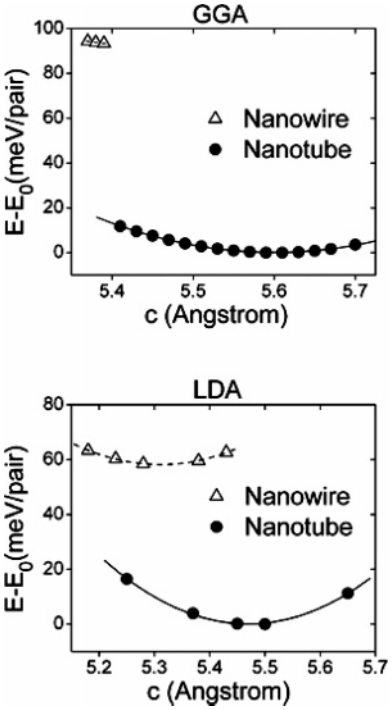

Figure 2. Energy vs c for 20 atom unit cell ZnO nanowire and SWZONT. (GGA and LDA). In GGA calculation, the nanowire relaxes into a nanotube when lattice parameter c is increased; in LDA calculation, the nanowire is metastable.

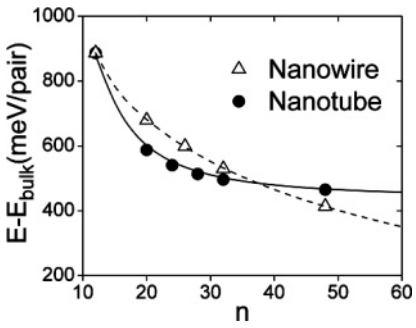

Figure 3. Relative energy for SWZONTs and nanowires from DFT results. The dashed line is just a guide to the eye that represents nanowires and converges to the ZnO bulk value. The solid line represents SWZONTs, is fitted to $1/n^2$, and converges to the graphene-like ZnO planar sheet.

diameter of a SWZONT is approximately proportional to n, so

$$E_{\text{strain}}(n) \approx c/n^2$$

By fitting DFT data points (see Figure 4, left panel), we obtain the strain energy:

$$E_{\text{strain}}(n) = 5.85 \times 10^4/n^2 \text{ meV/pair}$$

Therefore, the total energy of a SWZONT is

$$E_{\text{NT}}(n) = 440 + \frac{58\,500}{n^2} \text{ meV/pair}$$

The total energy of a ZnO nanowire can be approximated as

$$E_{\text{NW}}(n) = \frac{n_{\text{d}}}{n}E_{\text{d}} + \frac{n_{\text{b}}}{n}E_{\text{b}}$$

where E_{d} is the energy of a pair of Zn and O atoms with each having a dangling bond, E_{b} is the total energy of bulk ZnO, n_{d}/n and n_{b}/n are the fraction of atoms with and without dangling bonds. The value of n_{d} for some typical n are listed in Table 2. Taking $E_b = 0$ and fitting the DFT data (Figure 4, right panel), we get $E_{\text{d}} = 863$ meV/pair and the total energy of a ZnO nanowire is

$$E_{\text{NW}}(n) = \frac{n_{\text{d}}}{n}E_{\text{d}} = 863\,\frac{n_{\text{d}}}{n} \text{ meV/pair}$$

On the basis of the models above, the critical number of atoms when phase transition (nanotube to nanowire) occurs is $n \sim 40$, which agrees well with previous value $n \sim 38$, estimated directly from the DFT calculation.

Similar to the BN nanotube,[27] there is some buckling on the surface of the ZnO nanotube, i.e., the cylinder formed by O atoms has a larger diameter than the cylinder formed by Zn atoms (see Figure 1). It is shown in Figure 5 that, as the size of the SWZONT increases, the buckling distance ΔR (the radius difference of O and Zn cylinders) decreases as $1/n$ (or $1/R$) and eventually goes to zero when the tube becomes a flat sheet. This behavior is also observed in BN nanotubes, where it was explained by the different hybridizations of B and N atoms.[27,28] Here we offer a slightly different interpretation. Covalent bond-bending interactions try to keep the Zn and O cylinder radii R equal, with a restoring force $-k\Delta R$ per pair. The reason O atoms prefer a larger cylinder than Zn atoms is Fermi pressure. The HOMO levels are based on oxygen p orbitals. In common with free electrons, their energies increase toward the Fermi level because of increased kinetic energy to a value $E_{\text{F}} \propto \hbar^2[1/m_a\lambda_a^2 + 1/m_c\lambda_c^2]$ per pair, where the Fermi energy depends on m_a and m_c, band effective masses perpendicular and parallel to c, and λ_a and λ_c, the Fermi wavelengths in the two directions, which are fixed by the geometry of the atoms. Specifically, $\lambda_a \propto R/n$ and $\lambda_c \propto c$. Thus there is an outward force $-\text{d}E_{\text{F}}/\text{d}R \propto n^2/R^3 \propto 1/R$, where the last substitution follows because $n \propto R$. The force balance gives $\Delta R \propto 1/R \propto 1/n$, that is, the oxygen−zinc radial spacing falls off as $1/n$, as is seen roughly in Figure 5.

To make SWZONTs, they need to be very small. One way to do this is inhibiting radial growth by confinement of the SWZONT in a narrow cylindrical channel, as was done for ultrathin carbon nanotubes.[29] Extra-large pore zeolites such as VPI-5[30] might be used to control the size of SWZONTs. If ultrasmall catalyst particles can be made, a catalyst growth mechanism similar to ref 31 may also work for ZnO. The other growth strategy is to prevent the radial collapse of SWZONTs by growing them on the outer surface of other 1D nano structures such as metal nanowires (similar to ref 7) or carbon nanotubes (as suggested by ref 13).

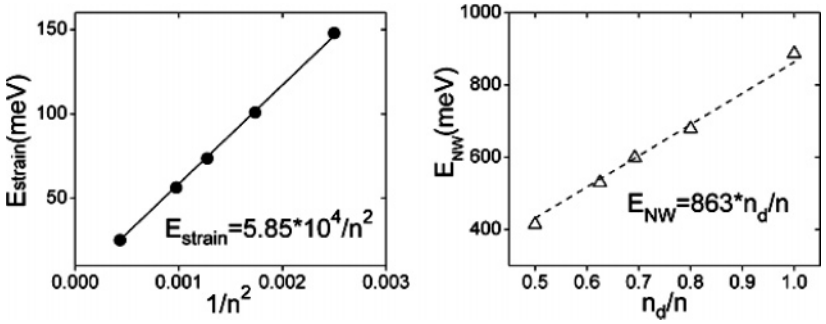

Figure 4. Fitting of the strain energy of SWZONT as a function of $1/n^2$ (left) and the ZnO nanowire energy as a function of n_d/n (right).

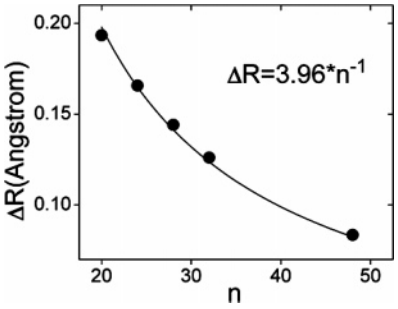

Figure 5. Buckling distance ΔR (the radius difference of O and Zn cylinders) vs the number of atoms per unit cell of a SWZONT. The solid line is a fit to $1/n$.

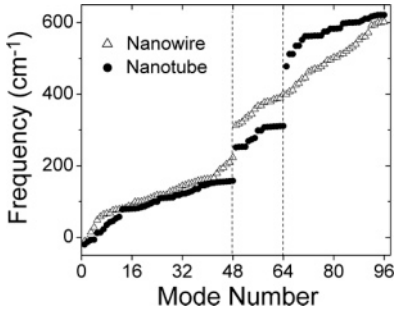

Figure 6. Phonon frequencies of all 96 modes at $q = 0$ for $n = 32$ nanowire and nanotube. The small negative frequencies of several lowest modes come from incomplete relaxation, tube−tube, or wire−wire interactions between periodic images and other uncertainties in the calculation. The gap around 250 cm^{-1} in the wire reflects the gap in mid-spectrum for vibrations in bulk ZnO.[32] The extra gap around 400 cm^{-1} in the tube occurs at exactly the $^2/_3$ point of the spectrum, where we believe the optical branches of the two-dimensional graphene-like ZnO sheet are split into $^1/_3$ lower lying perpendicular optic modes and $^2/_3$ higher lying parallel optic modes.

Table 2. Values of n_d for Some Typical n

n	12	20	26	32	48
n_d	12	16	18	20	24

In the present calculation, no foreign molecules passivate the surface, and all calculations are at zero temperature. In experiment, passivation may occur, and the temperature will be hundreds of Kelvin. Passivation favors the nanowire structure because the energy of the dangling bond gets lowered. High temperature favors the nanotube structure because it has larger vibrational entropy due to radial softness, which leads to low-frequency radial modes, especially a doubly degenerate very soft radial mode where the tube's cross section deforms into an ellipse. The total free energy lowering $T\Delta S$ for the $n = 32$ tube compared with the $n = 32$ wire is roughly $10k_BT$ with an uncertainty ~20%. This estimate uses the high-temperature formula $S_i \approx k_B \ln(k_BT/\hbar\omega_i)$ for the entropy of the ith harmonic oscillator, where $k_B \ln T$ is the classical answer, independent of frequency, and $-k_B \ln\omega_i$ is the quantum correction. Thus the free energy difference $\Delta F = F^{NT} - F^{NW}$ contains a term $-T(S^{NT} - S^{NW}) \approx k_BT \sum_i \ln(\omega_i^{NT}/\omega_i^{NW})$, which favors lower frequencies. The vibrational frequencies at $q = 0$ for $n = 32$ tube and wire (Figure 6), as calculated using Quantum Espresso, are used as ω_i. It is somewhat surprising how small the entropy enhancement is for the tube. To a large degree, in the optical branches (modes 49−96 in Figure 6), the softness of low-lying radial modes (49 to 64) of the tube is compensated by stiffness of the high-lying bond-stretching axial and tangential modes (65−96). In the acoustic branches, the softness is not compensated, and the free energy gets lowered.

Acknowledgment. We thank M. S. Hybertsen, M. R. Pederson, T. Sun, and L. L. Zhao for helpful discussions. Research at Brookhaven National Laboratory was supported by U.S. DOE under contract no. DE-AC02-98CH10886. Work at Stony Brook was supported by a BNL−Stony Brook Seed Grant. The ball−stick graphs are generated by the XCrysden graphical package.[33] Code available http://www.xcrysden.org/.

References

(1) Fan, Z.; Lu, J. G. *J. Nanosci. Nanotechnol.* **2005**, *5*, 1561.
(2) Wu, Y. Y.; Yang, P. D. *J. Am. Chem. Soc.* **2001**, *123*, 3165.
(3) Wang, Z. L. *J. Phys.: Condens. Matter* **2004**, *16*, R829.
(4) Zhang, J.; Sun, L.; Liao, C.; Yan, C. *Chem. Commun.* **2002**, *3*, 262.
(5) Wu, J. J.; Liu, S. C.; Wu, C. T.; Chen, K. H.; Chen, L. C. *Appl. Phys. Lett.* **2002**, *81*, 1312.
(6) Hu, J. Q.; Li, Q.; Meng, X. M.; Lee, C. S.; Lee, S. T. *Chem. Mater.* **2003**, *15*, 305.
(7) Zhang, X. H.; Xie, S. Y.; Jiang, Z. Y.; Zhang, X.; Tian, Z. Q.; Xie, Z. X.; Huang, R. B.; Zheng, L. S. *J. Phys. Chem. B* **2003**, *107*, 10114.
(8) Xing, Y. J.; Xi, Z. H.; Xue, Z. Q.; Zhang, X. D.; Song, J. H.; Wang, R. M.; Xu, J.; Song, Y.; Zhang, S. L.; Yu, D. P. *Appl. Phys. Lett.* **2003**, *83*, 1689.
(9) Kong, X. H.; Sun, X. M.; Li, X. L.; Li, Y. D. *Mater. Chem. Phys.* **2003**, *82*, 997.
(10) Kong, X. Y.; Ding, Y.; Wang Z. L. *J. Phys. Chem. B* **2004**, *108*, 570.
(11) Sun, Y.; Fuge, G. M.; Fox, N. A.; Riley, D. J.; Ashfold, M. N. R. *Adv. Mater.* **2005**, *17*, 2477.
(12) Erkoç, S.; Kökten, H. *Physica E* **2005**, *28*, 162.
(13) Tu, Z. C.; Hu, X. *Phys. Rev. B* **2006**, *74*, 035434.

(14) Wang; B. L.; Nagase, S.; Zhao, J. J.; Wang, G. H. *J. Phys. Chem. C* **2007**, *111*, 4956
(15) Baroni, S.; Dal Corso, A.; de Gironcoli, S.; Giannozzi, P. *Plane-Wave Self-Consistent Field*; http://www.pwscf.org.
(16) Vanderbilt, D.; *Phys. Rev. B* **1990**, *41*, R7892.
(17) Perdew, J. P.; Burke, K.; Ernzerhof, M. *Phys. Rev. Lett.* **1996**, *77*, 3865.
(18) Wöll, C.; *Prog. Surf. Sci.* **2007**, *82*, 55.
(19) Erhart, P.; Albe, K.; Klein A. *Phys. Rev. B* **2006**, *73*, 205203.
(20) Jaffe, J. E.; Snyder, J. A.; Lin, Z.; Hess, A. C. *Phys. Rev. B* **2000**, *62*, 1660.
(21) Kisi, E. H.; Elcombe, M. M. *Acta Crystallog.* **1989**, *C45*, 1867.
(22) *CRC Handbook of Chemistry and Physics*, 58th ed.; CRC: Boca Raton, FL, 1977.
(23) Desgreniers, S. *Phys. Rev. B* **1998**, *58*, 14102.
(24) *Landolt-Börnstein, Numerical Data and Functional Relationships in Science and Technology*; New Series, Group III, Vol. 17, Part b; Madelung, O., Ed.; Springer-Verlag: Berlin, 1982.
(25) Perdew, J. P.; Zunger, A. *Phys. Rev. B* **1981**, *23*, 5048.
(26) Robertson, D. H.; Brenner, D. W.; Mintmire, J. W. *Phys. Rev. B* **1992**, *45*, 12592.
(27) Blase, X.; Rubio, A.; Louie, S. G.; Cohen M. L. *Europhys. Lett.* **1994**, *28*, 335.
(28) Wirtz, L.; Rubio A.; de la Concha, R. A.; Loiseau, A. *Phys. Rev. B* **2003**, *68*, 045425.
(29) Wang, N.; Tang, Z. K.; Li, G. D.; Chen, J. S. *Nature* **2000**, *408*, 50.
(30) Davis, M. E.; Saldarriaga, C.; Montes, C.; Garces, J.; Crowder, C. *Nature* **1988**, *331*, 698.
(31) Hafner, J. H.; Bronikowski, M. J.; Azamian, B. R.; Nikolaev, P.; Rinzler, A. G.; Colbert, D. T.; Smith, K. A.; Smalley, R. E. *Chem. Phys. Lett.* **1998**, *296*, 195.
(32) Serrano, J.; Romero A. H.; Manjón, F. J.; Lauck R.; Cardona M.; Rubio A. *Phys. Rev. B* **2004**, *69*, 094306.
(33) Kokalj, A., *J. Mol. Graphics Modell.* **1999**, *17*, 176.

NL070788K